Analysis of Digital System Performance in EAM-Based Photocurrent Driven Wavelength Converter

Matthew N. Sysak, *Member, IEEE*, James W. Raring, *Member, IEEE*, Matthew Dummer, *Student Member, IEEE*, Henrik N. Poulsen, *Member, IEEE*, Daniel J. Blumenthal, *Fellow, IEEE*, and Larry A. Coldren, *Fellow, IEEE*

***Abstract*—This work describes the factors that influence the digital system performance of a monolithically integrated photocurrent driven wavelength converter. For an optimized input power to the receiver section of the device, experiments show <1-dB power penalty for conversion between 1548 and 1563 nm at 10 Gb/s. Under optimized conditions, performance is limited by the output extinction ratio of the converted signals.**

***Index Terms*—Monolithic integration, photonic integrated circuits, wavelength converters.**

I. Introduction

PHOTONIC integrated circuits that are capable of wavelength switching and signal regeneration are critical components for extending the reach of present day optical networks. Several devices are currently available that can perform these functions. These include semiconductor optical amplifiers (SOAs) that utilize cross-gain modulation or cross-phase modulation, electroabsorption modulators (EAMs) based on photocurrent effects, and fiber-based wavelength converters that employ wave mixing [1]. Of these approaches, small form factor wavelength switching elements that are compatible with monolithic integration offer additional benefits, such as low optical coupling losses between components and reduced packaging costs.

Recently, we have demonstrated a monolithically integrated photocurrent driven wavelength converter (PD-WC) that can perform signal regeneration. The device is compatible with a range of input and output wavelengths, and does not require optical filtering to separate input and converted signals [2]. The wavelength converter is based on the dual-quantum-well (QW) integration platform where fabrication requires a single blanket InP regrowth in combination with simple selective wet etching steps to form optical gain and passive routing/EAM regions [3]. The device utilizes photocurrent driven technology where an optically preamplified receiver drives an EAM that is part of a tunable optical transmitter. Similar devices based on this principle have been demonstrated at bit rates of 500 Gb/s [4].

Manuscript received August 29, 2006; revised November 2, 2006. This work was supported by Defense Advanced Research Projects Agency (DARPA)/MTO CS-WDM under Grant N66001-02-C-8026 and by Intel Corporation under Grant TXA001630000.

The authors are with the Department of Electrical Engineering and the Department of Materials, University of California Santa Barbara, Santa Barbara, CA 93116 USA (e-mail: mnsysak@engineering.ucsb.edu).

Digital Object Identifier 10.1109/LPT.2006.888954

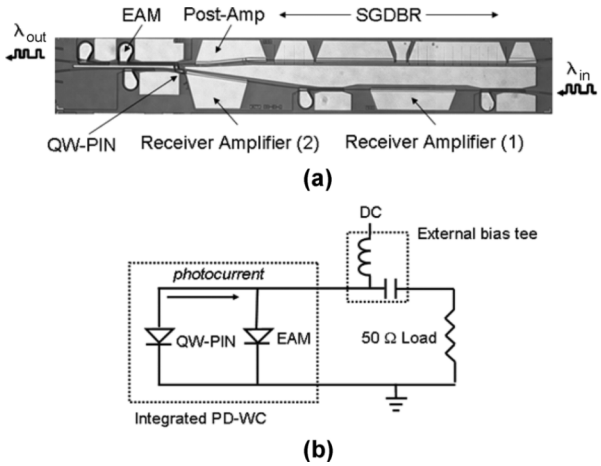

Fig. 1. (a) Scanning electron micrograph (SEM) of the PD-WC. (b) Circuit schematic for PD-WC operation.

In this work, we use bit-error-rate (BER) measurements to optimize the digital system power penalty through the wavelength converter. Under optimum conditions, the PD-WC does not introduce significant noise or jitter onto the wavelength-converted signals. Furthermore, when optimized, the power penalty through the wavelength converter is limited by the converted signal extinction ratio (ER).

II. Device Overview

A schematic of the PD-WC along with an equivalent circuit for device operation is shown in Fig. 1. The device consists of a monolithically integrated optical receiver section and widely tunable transmitter section. The receiver is comprised of a 600-μm-long straight waveguide SOA that is 3-μm-wide (receiver amplifier 1) and a 400-μm-long flared waveguide SOA (receiver amplifier 2). The second SOA waveguide width is exponentially flared from 3 to 12 μm along the length of the device. A linearly tapered $(12-3\ \mu\text{m})$ waveguide QW-PIN photodetector follows the flared SOA [5].

The transmitter section of the PD-WC consists of a four-section sampled-grating distributed Bragg reflector (SGDBR) laser, a 550-μm-long postamplifier SOA, and a 400-μm-long EAM. A voltage source and a bias tee are used to simultaneously reverse bias both the QW-PIN and the EAM, and a 50-Ω load resistor is used to enhance the bandwidth. An equivalent circuit for the device is shown in Fig. 1(b). A 35-μm-long metal interconnect routes the photocurrent generated in the QW-PIN to the EAM and the load resistor, where the resulting voltage drop changes

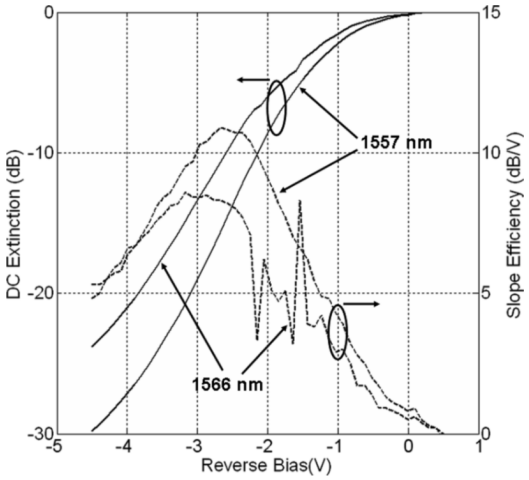

Fig. 2. DC extinction (solid line) and slope efficiency (dashed line) results for a 400-μm EAM at output wavelengths of 1557 and 1566 nm.

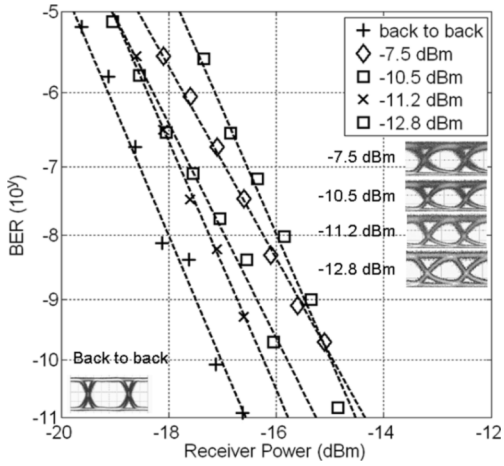

Fig. 3. BER curves for various input powers to the integrated receiver in the PD-WC. The input wavelength is 1548 nm, the input extinction is 15 dB, and the output wavelength is 1563 nm.

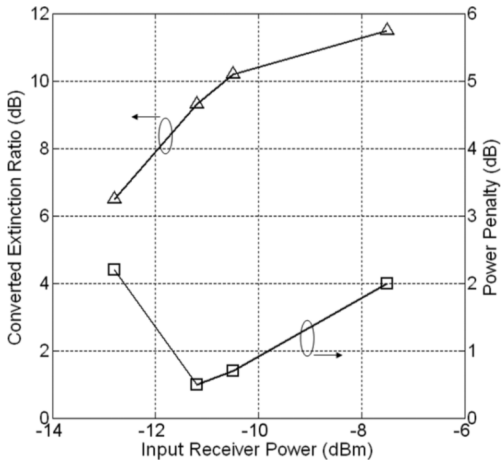

Fig. 4. Summary of BER measurements for various input powers to the PD-WC receiver. Input and output wavelengths are 1548 and 1563 nm, respectively, and applied reverse bias is -3 V.

the transmission properties of the EAM. This writes the signal from the receiver to the output wavelength of the transmitter. For transverse electric (TE) polarized signals, the receiver gain is 20 dB with a current density of 6 kA/cm^2 applied to both SOAs. The receiver exhibits a 1-dB gain compression at -7-dBm input power, and has a sensitivity $(\text{BER} = 10^{-9})$ of -18.5 dBm at 10 Gb/s for an input wavelength of 1548 nm.

III. Experiment

To optimize the performance of the PD-WC, a set of two BER measurements were performed using nonreturn-to-zero (NRZ) data at 10 Gb/s. The NRZ data contained a $2^{31}-1$ pseudo-random bit sequence. The experimental setup was the same as in [2], where an optical signal at 1548 nm with a 15-dB ER was fed to the PD-WC receiver. The polarization of the input signal was optimized using a polarization controller, and was selected for maximum gain in the integrated receiver. The compressively strained QWs used for optical gain in the PD-WC render the receiver SOAs highly polarization-sensitive, with preferential gain for TE guided modes. This issue could be circumvented by including an additional regrowth in the fabrication process, where an optimized bulk active region could be grown and subsequently removed for the receiver amplifiers similar to that employed for high-speed photodetectors in [6].

The first set of BER measurements was used to determine an optimum input power level for the PD-WC. BER curves were generated for back-to-back (without the device) and wavelength-converted signals for a range of input powers to the integrated PD-WC receiver. The optimum input power was defined as where the power penalty, measured as the difference in receiver power (the receiver in the test setup) between back-to-back and converted signals at a BER of 10^{-9}, was minimized. In these experiments, the output wavelength from the PD-WC was fixed at 1563 nm and the reverse bias conditions were set to -3 V to achieve maximum EAM slope efficiency. The DC extinction and slope efficiency of the EAM for wavelengths of 1566 and 1557 nm are shown in Fig. 2. The receiver SOAs are biased at 6 kA/cm^2 and the SGDBR gain and postamplifier SOA are biased at 100 mA.

To further optimize the PD-WC performance, a second set of BER measurements was performed for various QW-PIN/EAM reverse bias conditions. The input power to the device was fixed based on the results from the first set of BER measurements and the output wavelength from the PD-WC was again 1563 nm. The bias conditions for the receiver SOAs, transmitter SOA, and the SGDBR are identical to that in the first set of measurements.

IV. Results

Results from the first set of BER measurements are shown in Fig. 3 along with wavelength-converted eye diagrams for fiber coupled receiver input powers of -12.8, -11.2, -10.5, and -7.5 dBm. All eye diagrams are clear and open indicating that jitter through the PD-WC is not significant. The input and output optical signal-to-noise ratios (OSNRs) in these experiments was >30 dB, which is well above the region where OSNR limits BER. For increasing optical power to the PD-WC, Fig. 3 shows that the power penalty initially decreases, then increases. The power penalty through the device as a function of input power and output ER from the wavelength converter are shown in Fig. 4. At low input powers (-12.8 dBm), increasing optical power to the integrated receiver increases the photocurrent from the QW-PIN, which generates a larger voltage across the

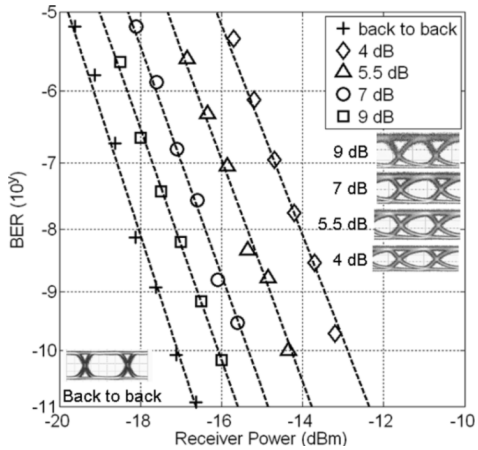

Fig. 5. BER measurements for QW-PIN/EAM reverse biases of −2, −2.3, −2.7, and −3 V. Wavelength converted ERs at these biases are 4, 5.5, 7, and 9 dB, respectively.

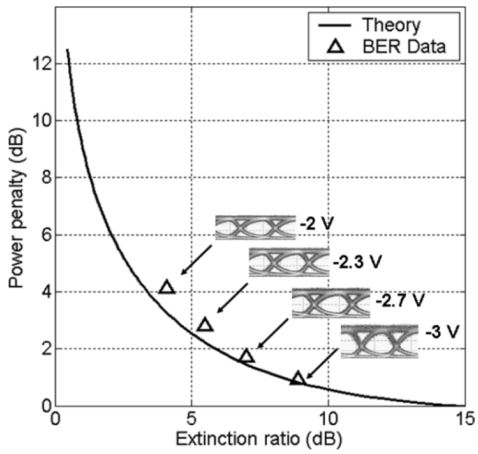

Fig. 6. Theoretical power penalty versus ER and experimental data for wavelength conversion from 1548 to 1566 nm. Applied reverse bias conditions are −2, −2.3, −2.7, and −3 V.

load resistor. The larger voltage swing drives the EAM through greater changes in transmission, improving the output extinction of the device. However, as the input power to the receiver increases beyond −11.2 dBm, the power penalty begins to increase despite improvements in output ER. This increase originates from a change in slope in the BER curves shown in Fig. 3, and is indicative of modified noise statistics in the wavelength-converted signals. The changing noise distribution most likely results from pattern-dependent gain overshoot and recovery in the receiver SOAs [8], which can be seen as "one" noise in the eye diagrams in Fig. 3 for power levels > -10.2 dBm. Based on minimizing the power penalty through the device, the optimal input power to the PD-WC is −11.2 dBm. Under these conditions, the clear eye diagrams and the parallel BER slopes between back-to-back and converted data indicates that device performance is not limited by jitter or pattern dependence generated in the PD-WC receiver.

Results from the second set of BER measurements, which investigates how changing the wavelength converter bias effects digital system performance, are shown in Fig. 5. For reverse biases of −2.0, −2.3, −2.7, and −3 V, wavelength-converted signals show ERs of 4, 5.5, 7, and 9 dB, respectively. Eye diagrams are included for the wavelength-converted signals at each of the examined bias conditions. The increase in ER as a function of bias comes from the increasing EAM slope efficiency shown in Fig. 2. From Fig. 5, as the ER improves, there is a clear reduction of the power penalty between back-to-back and converted signals. To determine if the output ER from the PD-WC limits BER performance, the extracted power penalty through the wavelength converter is compared with theory from [7] in Fig. 6. The theoretical predictions are based on the increase in receiver power (the receiver used to measure BER) that would be required to achieve a BER of 10^{-9} given a range of signal ERs. To convert the increased receiver power to a power penalty through the device, a constant is subtracted from the theoretical predictions to account for the 15-dB ER in the input signal to the PD-WC. The excellent agreement between the predictions and data indicates that under these optimized input power conditions, converted signal ER limits device performance.

V. Conclusion

We have demonstrated that the digital system performance of the PD-WC can be limited by the ER of the converted signals at 10 Gb/s. Under optimized input conditions, the bias across the EAM and QW-PIN can be changed to achieve less than 1-dB power penalty through the device. By improving receiver saturation or EAM efficiency in the PD-WC, the converted ER could be improved, leading to lower power penalties and a larger dynamic range.

References

[1] S. B. Yoo, "Wavelength conversion technologies for WDM network applications," *J. Lightw. Technol.*, vol. 14, no. 6, pp. 955–966, Jun. 1996.

[2] M. N. Sysak, J. W. Raring, L. A. Johansson, H. N. Poulsen, J. S. Barton, D. J. Blumenthal, and L. A. Coldren, "Optical 2R and 3R regeneration with dynamic wavelength switching using a monolithically integrated, widely tunable photocurrent driven wavelength converter," in *Eur. Conf. Optical Commun. (ECOC)*, Cannes, France, Sep. 2006.

[3] M. N. Sysak, J. W. Raring, J. S. Barton, M. Dummer, D. J. Blumenthal, and L. A. Coldren, "A single regrowth integration platform for photonic circuits incorporating tunable SGDBR lasers and quantum well EAMs," *IEEE Photon. Technol. Lett.*, vol. 18, no. 15, pp. 1630–1632, Aug. 1, 2006.

[4] S. Kodama, T. Yoshimatsu, and H. Ito, "500 Gbit/s optical gate monolithically integrating photodiode and electroabsorption modulator," *Electron. Lett.*, vol. 40, no. 9, pp. 555–556, Apr. 2004.

[5] A. Tauke-Pedretti, M. Dummer, J. S. Barton, M. N. Sysak, J. W. Raring, and L. A. Coldren, "High saturation power and high gain integrated receivers," *IEEE Photon. Technol. Lett.*, vol. 17, no. 10, pt. 10, pp. 2167–2169, Oct. 2005.

[6] J. W. Raring, E. J. Skogen, C. S. Wang, J. S. Barton, G. B. Morrison, S. Demiguel, S. P. Denbaars, and L. A. Coldren, "Design and demonstration of novel QW intermixing scheme for the integration of UTC-type photodiodes with QW-based components," *IEEE J. Quantum Electron.*, vol. 42, no. 2, pp. 171–181, Feb. 2006.

[7] G. P. Agarwal, *Fiber Optic Communication Systems*. New York: Wiley, 1997, p. 169.

[8] K. Morito, M. Ekawa, T. Watanabe, and Y. Kotaki, "High-output-power polarization-insensitive semiconductor optical amplifier," *J. Lightw. Technol.*, vol. 21, no. 1, pp. 176–181, Jan. 2001.